第 22 卷第 5 期 半 导 体 学 报 Vol. 22, No. 5
2001 年 5 月 CHINESE JOURNAL OF SEMICONDUCTORS May, 2001

Quantum Well Infrared Photodetectors: the Basic Design and New Research Directions

H. C. Liu

(*Institute for Microstructural Sciences National Research Council, Ontario K1A 0R6, Canada*)

Abstract: The basic design principles and parameters of GaAs/AlGaAs quantum well infrared photodetectors (QWIP) are reviewed. Furthermore new research directions, devices and applications suited for QWIPs are discussed. These include monolithic integration of QWIPs with GaAs based electronic and optoelectronic devices, high frequency and high speed QWIPs and applications, multicolor and multispectral detectors, and p-type QWIPs.

Key words: quantum well; infrared; photodetector; high speed; high frequency; multicolor; multispectral
EEACC: 7230C
CLC number: TN215 **Document code**: A **Article ID**: 0253-4177(2001)05-0529-09

1 Introduction

The physics[1] and applications[2] of quantum well infrared photodetectors (QWIP) based on GaAs/AlGaAs materials are well established. Thermal infrared (IR) imaging is the main existing application of QWIPs fabricated into focal plane arrays[2]. In this case, QWIPs are used for detecting weak signals and the device parameters are chosen to achieve the highest possible detection sensitivity (detectivity) and background limited infrared performance (BLIP) temperature. The design principals for this existing application are discussed in detail in Ref. [1]. In this overview paper, we first review the design principals and present the parameters for optimized QWIPs, and then introduce several directions for future research and development.

A standard QWIP consists of multiple quantum wells with contacts on either sides. The operation of a photoconductive QWIP is easily summarized using the bandedge profile shown in Fig. 1 (above). Upon application of a bias voltage, incide-

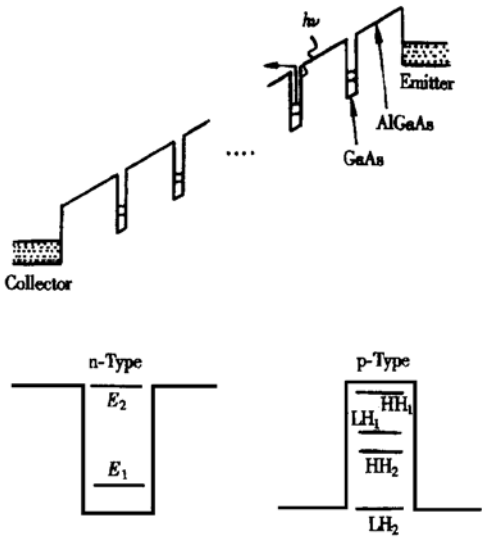

FIG. 1 Bandedge Profile of Quantum Well Infrared Photodetector Under Bias (Above) Because of the unipolar nature of the device, we label the two contacts as emitter and collector. The lower part shows a n-type (left) and p-type (right) quantum well.

H. C. Liu male, Member of Overseas Advisory Committee of Chinese Journal of Semiconductors, Guest Professor of Institute of Semiconductors (CAS), Shanghai Institute of Technical Physics (CAS), Beijing Polytechnic University, and Lanzhou University.

Received 16 February 2001

nt photons excite electrons out the quantum wells creating a photocurrent. The wells are doped to provide a population of electrons in the ground state subbands. The lower-left part of Fig. 1 shows the energy levels for a n-type quantum well. Similarly, the QWIP structure may be p-type with both heavy hole (HH) and light hole (LH) states (lower-right part of Fig. 1 discussed in Sec. 6)

2 QWIP Design and Parameters

Given the substantial research on QWIPs over the past decade, especially those based on GaAs/AlGaAs, the basic design and operation principles are reasonably understood for a standard photoconductive QWIP. In this section, we summarize the guidelines in designing an optimum photoconductive QWIP, which involves choosing the following parameters: well width L_w, barrier height V_b, barrier width L_b, well doping density resulting a two-dimensional (2D) carrier density N_D, and number of wells N. We concentrate on the simplest structure made of GaAs/AlGaAs square quantum wells. The well region is GaAs, and the barrier is $Al_xGa_{1-x}As$ so that its height is controlled by Al fraction x.

In this section we discuss n-type QWIPs. It has been well established[1] that the optimum well shape is the one having the first excited state in resonance with the top of the barrier. Given this design rule, the well width and barrier height are fixed once an desired detection wavelength (peak wavelength λ_p) is chosen. Figure 2 shows these parameters for a range of λ_p for a GaAs/AlGaAs quantum well. The peak detection wavelength λ_p corresponds to the energy difference between the first excited and the ground states. The calculation is a simple one-band effective mass model calculation. The barrier height V_b relates to Al fraction by $V_b = 0.87 \times x$ eV. All higher order effects have been neglected, such as, band non-parabolicity, Coulomb interaction between ionized donors and electrons (Hartree correction), exchange-correction effect, and depolarization-exciton effect. For a structure appropriate for $\lambda_p = 10\mu m$ these effects all lead to a modification of the transition energy in the few-percent range. A detailed review of these effects is found in Ref. [3]

As an example, the main effect of exchange-correlation and depolarization-exciton is to shift the transition energy to a higher value. The amount is about 10meV for a 2D electron density of $N_D = 5 \times 10^{11} cm^{-2}$. Taking this into account, the renormalized peak wavelengths are shown in Fig. 2 in parentheses. The effect is not very important for short wavelength structures, but is dramatic for long wavelengths. In general, longer than about $20\mu m$, Hartree, exchange-correlation, and depolarization-exciton effects must be included to obtain good fit to experiments. Shorter than about $7\mu m$, the non-parabolicity effect becomes important.

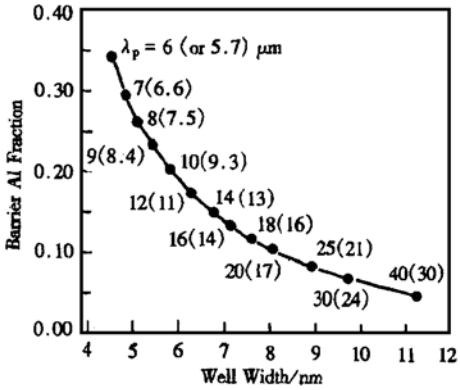

FIG. 2 Optimum n-Type GaAs/AlGaAs QWIP Calculated Parameters of Barrier Al Fraction and Well Width for Given Peak Detection Wavelength(λ_p) Including many-body effects, the values in parentheses are for a quantum well with doping density of about $5 \times 10^{11} cm^{-2}$.

The next parameter is the well doping. Either uniform doping or δ doping are employed, which give essentially the same result. Growth conditions should be chosen so that the doping migration into the barriers is minimized[4,5]. To maximize the detector limited detectivity, without going through the argument[1], the doping density should be such that the Fermi energy is $E_f = 2k_BT$, where T is the

desired operating temperature. On the other hand, to maximize the BLIP temperature, one should have $E_f = k_B T$. The doping density relates to Fermi energy by $N_D = (m/\pi\hbar^2) E_f$. Figure 3 shows these two (trivial) relations for n-type QWIPs with GaAs wells.

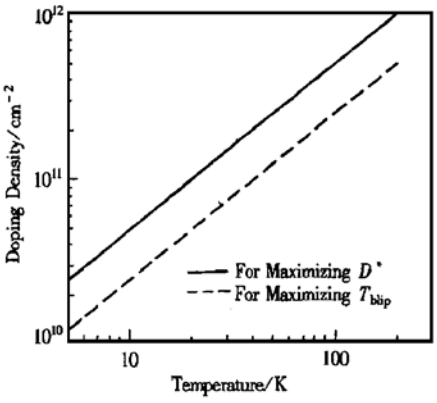

FIG. 3 Optimum n-Type Doping Density Versus Device Operating Temperature
The well material is GaAs.

The author has not found an intuitive way to choose the barrier width. Generally speaking, the barrier width should be wide enough so that the inter-well tunneling current is suppressed. There is a critical value beyond which any further increase in L_b does not lead to a lowering in dark current for a given applied field. This means that one should use thick barriers. On the other hand, the practical epitaxial growth is such that the thicker the total layer the lower the material quality. Furthermore, if the barrier width can be reduced, one can grow more repeats for higher absorption for a given total epi-layer thickness. Empirically, a barrier width in the range of 30 to 50nm seems to be sufficient. A systematic study[6] on a set of QWIPs operating in the 8—10μm region concluded that L_b should be larger than 20nm for 2π background and 77K operation and 30nm for F/2 background and 70K operation. More systematic experimental and modeling studies are desired.

Last, for the number of wells or repeats, since the absorption depends strongly on the device geometry and optical coupling scheme, only a general guideline can be given: one should maximize the absorption with a minimum number of wells.

As a final note: These design guidelines are based on our current understanding and on our and other published experiments. There have been very limited systematic studies to re-enforce/confirm these design "rules".

3 Imaging Devices by Monolithic Integration and Optical Readout

A distinctive advantage of GaAs-based QWIPs, yet to be fully utilized, is the potential of monolithic integration with electronic and optoelectronic devices and circuits. Though far less advanced than Si-based devices and circuits, GaAs-based high electron mobility transistor (HEMT) and heterojunction bipolar transistor (HBT) are reasonably well developed. Recently, a very interesting proof-of-the-concept demonstration has been reported[7], where QWIPs have been monolithically integrated with HEMTs for read-out in an array format. QWIPs have also been envisioned to be integrated with HBTs for array read-out[8]. The monolithic integration is clearly an extremely promising research direction and deserves a lot more attention than in the past so far.

Another unique feature is the ability to integrate with optoelectronic devices. We have been investigating the integration of QWIPs with light emitting diodes (LEDs) for optical read-out. The basic idea[9] of an integrated QWIP-LED is to epitaxially grow a QWIP and a LED on top of each other. The QWIP can be either n- or p-type. Figure 4 shows a GaAs/AlGaAs n-QWIP with an InGaAs/GaAs quantum well LED. Only two contacts are made — to the heavily p-doped LED contact layer and the heavily n-doped QWIP emitter. QWIP is a photoconductor so that under IR illumination its resistance decreases, which leads to an increase in the voltage drop across the LED and therefore an increase in the LED light emission. This device is therefore an IR to LED light con-

verter. For 77K operation, a well-designed QWIP can be very efficient[10] with easily higher than 10% absorption, and the LED technology is well developed. An optimized QWIP-LED therefore can be very efficient with little or no loss of performance compared with the QWIP alone used as a detector. However, the advantage of this integrated QWIP-LED is of importance technologically. In this scheme, one can make large format 2D imaging devices without the need of making any circuits on the device chip and without the need of hybrid bonding with another readout chip (normally a Si IC). The resulting LED emission can be easily imaged using the well-developed Si-CCD. The first experimental demonstration of QWIP-LED was reported in Ref. [9]. The concept was independently proposed by Ryzhii *et al*[11].

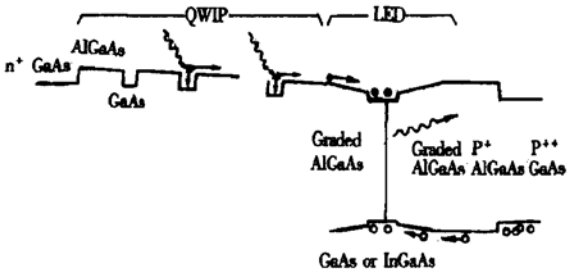

FIG. 4 Bandedge Profile of Integrated QWIP with LED For the QWIP part, only the conduction bandedge is shown. A forward bias is applied so that both the QWIP and the LED are in operating conditions. Photocurrent electrons from the QWIP recombine with injected holes in LED, giving rise to an increase in LED emission.

An intriguing possibility for QWIP-LED is to fabricate a continuously image conversion device — a pixelless large-area imaging device[12]. The idea is that since the entire active layer of a QWIP-LED in the growth direction is very thin (normally less than 4μm) the up-conversion process (i. e., photoexcitation in QWIP, carrier transport to LED, and radiative recombination in LED) should have little in-plane spreading. Theoretical analyses[13,14] show that the intrinsic spreading and crosstalk are negligible for a practical QWIP with a large number of wells, supporting the pixelless concept. The first demonstration of the pixelless QWIP-LED used a p-type QWIP for the simplicity of avoiding the fabrication of a grating[15]. An n-type device has also been demonstrated[16]. Currently we are working towards an optimized large-area pixelless imaging device. The concept of up-conversion may be expanded to cover the technological important region of 1.5μm[17].

4 High Speed QWIPs

Another distinctive advantage of QWIPs over standard detectors made of HgCdTe is their intrinsic high speed. High frequency and high speed detectors may create new applications, for example, environmental remote sensing of molecules[18] and CO_2 laser based (or other long wavelength laser based) communication, as well as laboratory use[19,20]. The intrinsic high speed capability is related to the inherent short carrier lifetime $\tau_{life} \approx 5$ps (30GHz) as inferred by our experiments[21,22]. For these applications, it is common that there is a strong signal or a powerful local oscillator. In such a case, a high dark current can be tolerated, and a high absorption and high operating temperature is desirable. Note also that since the applications discussed here commonly use lasers, the polarization sensitivity of the n-type QWIP is no longer a disadvantage. In this section, we discuss simple ways to improve absorption and to aim for near room temperature[23] operation.

Starting from the standard QWIP structure, the simplest way to improve absorption is to dope the wells more heavily and to employ more wells. Three QWIP wafers were grown in a VG molecular beam epitaxy system. The main difference between the samples is the well doping density. The period of the 100-repeat multiple quantum well structure consists of a GaAs well and $Al_xGa_{1-x}As$ barriers. The GaAs well center region is doped with Si to 1×10^{12}, 1.5×10^{12}, and 2×10^{12} cm^{-2}, respectively. The well width is 6.6, 6.6 and 5.9nm, the barrier width is 25.0, 25.0 and 24.0nm, and the Al frac-

tion is 0.200, 0.192 and 0.197, respectively, for the three samples. The top and bottom GaAs contact layers are 400 and 800nm thick, doped with Si to $2\times10^{18}cm^{-3}$. Mesa devices were fabricated by standard GaAs processing techniques. All devices were packaged into the 45° edge facet geometry[24] for optical coupling.

With increasing well doping, the device dark current increases rapidly. Measurements of BLIP temperature (T_{BLIP}) show that T_{BLIP} is degraded with increasing doping and $T_{BLIP}\approx60$, 45 and 30K for 1×10^{12}, 1.5×10^{12}, and $2\times10^{12}cm^{-2}$ doping, respectively. This clearly indicates that these devices are far from optimum for low signal applications. They do however have high absorptions. At 45° incident and for polarized light, the absorption per quantum well per pass is about 0.54% for a standard 10μm QWIP with $5\times10^{11}cm^{-2}$ doping per well[1]. For a doping density of $1.5\times10^{12}cm^{-2}$, the one-well/one-pass absorption is expected be about $\eta_1\approx1.6\%$. If a 90% absorption is desired, the number of wells N needed is determined by: $\exp(-2N\eta_1=10\%$, which gives $N=72$. (The factor of 2 in the exponential takes into account the double passes in a 45° facet detector geometry.) This is why we have chosen $N=100$ to ensure high (>90%) absorption. Measurements at both Brewster angle and 45° incidence indeed show the expected behavior. The present set of QWIPs is designed to cover the 10.3 and 10.6μm branches of the CO_2 laser. Figure 5 show the spectral response curves for the three samples. It is noted that as the doping is increased the spectrum is broadened. As the absorption in the $1.5\times10^{12}cm^{-2}$ doping sample is sufficient, we conclude that such a structure is near the optimum.

As stated before in Sec. 2, the condition $E_f=2k_BT$ maximizes the detector sensitivity (see Fig. 3). It is then expected that the doping range of $(1-2)\times10^{12}cm^{-2}$ should lead to QWIPs operating near room temperature albeit with a reduced sensitivity. Measured results at various temperatures using a CO_2 laser tuned to 10.6μm are shown in Fig. 6. It is clear that the device does work up to room temperature.

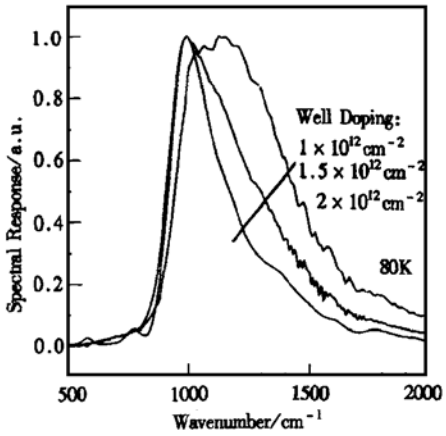

FIG. 5 Spectral Response Curves at 80K for the Three 100-Well QWIPs

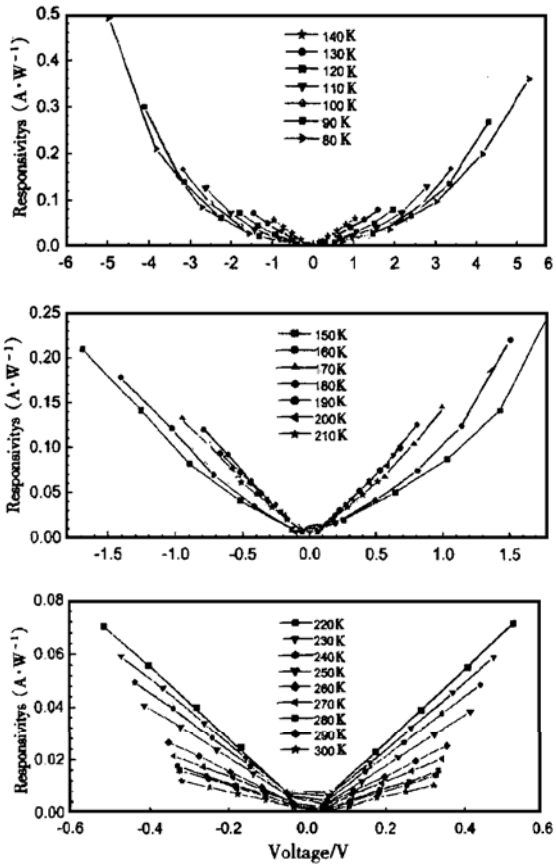

FIG. 6 Measured Responsivity for 1.5×10^{12} Doping QWIP Under CO_2 Laser Illumination and at Various Temperatures

At present time, QWIPs hold the unique position of having high speed/frequency capability and high absorption for the thermal infrared region. There are no competitive alternatives. It is also possible to go even higher (> 30GHz) by, for example, reducing the barrier width so that the inter-well tunneling becomes the main transport mechanism.

5 Multicolor and Multispectral QWIPs

Being based on thin multilayers grown by epitaxial techniques, the design of QWIPs is very flexible. This enables various implementations of multicolor and multispectral detectors. In general, a multicolor or multispectral detector is a device having its spectral response varied with parameters like voltages or any other parameters such as pressure, magnetic field, filter position, and so on. The latter cases are not as desirable in practical applications and are not discussed here.

The most direct approach involves contacting each intermediate conducting layer separating one-color QWIPs grown in a multistack. This results in a separately readable and addressable multicolor QWIP with multiple-electrical leads, and a two-color version has been reported[25]. The advantage of this approach is its simplicity in design and its negligible electrical cross-talk between colors. The drawback is the difficulty in fabricating a many color version because of the many separate leads required in contacting each intermediate layer. Bois *et al.*[26,27] have developed processing technologies for implementing two-color imaging arrays.

Another approach is to have a QWIP with a switchable response, e. g., for an applied voltage V_1 the response is at λ_1 and for V_2 at λ_2. One such example is realized by stacking the usual one-color QWIPs separated by thin conducting layers[28,29]. We rely on the highly non-linear and exponential nature of the device dark current-voltage characteristics. This implies that an applied voltage across the entire multistack would be distributed among the one-color QWIPs according to their values of dc resistances. Thus, when the applied voltage is increased from zero, most of the voltage will be dropped across the one-color QWIP with the highest resistance. As the voltage is further increased, an increasing fraction of the voltage will be dropped across the next highest resistance one-color QWIP, and so on. Since the detector responsivity of a one-color QWIP gradually turns on with applied voltage, we therefore can achieve a multicolor QWIP with spectral response peaks that turn on sequentially with applied voltage. The advantage of this approach is that it is simple in fabrication (as it requires only two terminals) and suited for implementing a QWIP with many colors. The drawback is the difficulty to achieve a negligible electrical crosstalk between colors.

The last case is a QWIP with its response continuously tuned in a range of wavelengths. The demonstrated examples of this approach involve special shapes of quantum wells, e. g., a stepped well[30] so that the response spectrum shifts as a function of applied bias voltage. This provides a continuous tuning of the spectrum by moving the intersubband resonance position. A range from 8.5 to 13.5μm has been achieved using stepped wells[30]. The large continuous tuning capability is the distinct feature of this approach. The difficulty is to ensure a good QWIP performance for all voltages. To achieve a good performance, the transition final state (usually the first excited state) must be close to the top of the barrier, as discussed before, providing a large intersubband transition strength and, at the same time, an easy escape for the excited carriers. These two conditions are difficult to fulfill for all voltages.

For some applications, it is desirable to have a multispectral detector covering not only the middle or far infrared but also the visible or near infrared spectral regions. We have investigated dual-band operation of InGaAs/InP QWIPs for both near infrared (NIR) and middle infrared (MIR) spectra and GaAs/AlGaAs QWIPs for visible (VIS) and

middle infrared. The idea of dual-band operation of an InGaAs/InP QWIP is straightforward[31]. A usual QWIP structure with InGaAs wells and InP barriers is used for MIR detection. At the same time, NIR can be absorbed in the InGaAs layers resulting in a photocurrent. The contact layers are made of InP so that the NIR light can reach the quantum well region without being absorbed. For dual-band detection using conventional GaAs/AlGaAs QWIPs, a small modification is needed[32]: the GaAs top contact is replaced by a large bandgap layer which opens a window for visible light to reach the quantum-well region. In both cases, reasonable detector performance was obtained, and the details were reported in Refs. [31, 32]. Although these devices provide MIR/FIR and VIS/NIR detection only in a simultaneous mode, the simplicity is its advantage. Similar idea can be applied to other systems such as InGaN/GaN for infrared and ultra-violet dual-band detection. An alternative approach for dual-band detection was reported by Schneider *et al.*[33] involving a stacked QWIP and p-i-n diode, which has a performance advantage since two devices can be separately optimized for MIR and NIR.

As a final comment on multicolor and multispectral devices, it seems that for all the approaches the device performance has not been fully optimized. Further work is therefore needed both in optimization and in new and better designs. Moreover, multicolor QWIPs require special gratings which have not been studied. One possibility is to use quasi-random gratings[34,35].

6 P-QWIPs

The attractive feature of p-QWIPs comes from the elimination of the need for a grating coupler. This provides a significant simplification in the fabrication of a large focal plane array. To realize the potential advantage of a strong absorption under normal incidence, we have carried out a series of optimization studies. By systematically optimizing the valence band structure[36,37], the 2D well doping density[38], and the barrier thickness[39], we have shown that p-type GaAs/AlGaAs QWIPs are now at a stage with performance comparable to their n-type counterparts. We have demonstrated that to achieve an optimal p-QWIP for normal incident detection one should employ the first heavy hole (HH1) to second light hole (LH2) transition with LH2 in resonance with the top of the barrier. The calculated optimum quantum well parameters are shown in Fig. 7. Here the barrier height is taken to be $0.53 \times x$ eV. Because of the non-parallel subband dispersion, intersubband transition in p-type quantum wells displays a broader spectrum than that for n-type. The optimum 2D well doping density is found to be around $2 \times 10^{12} cm^{-2}$, which maximizes the BLIP temperature (reaching about 100K for 5μm cutoff devices) as well as the dark current limited detectivity. For a 3—5μm device, the optimum barrier width is about 20nm, which is the minimum thickness for suppressing interwell tunneling.

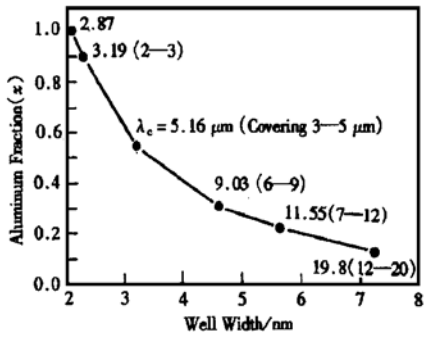

FIG. 7 Optimum p-Type GaAs/AlGaAs QWIP Calculated Parameters (Courtesy of F. Szmulowicz) of Barrier Al Fraction and Well Width for Given Cutoff Wavelength (λ_c) The values in parentheses give the spectral ranges covered.

Although the performance of the optimized p-QWIPs is quite good in term of BLIP temperature and detectivity, etc., the absorption quantum efficiency per quantum well is still quite low. To improve quantum efficiency, a direct way is to use more quantum wells. We investigated another approach for improving the quantum efficiency of p-

QWIPs[40]. By using microcavity the peak absorption and thus the peak responsivity can be significantly increased. The cavities are fabricated by applying thick gold films on the detector bottom sides after substrate removal via selective wet etching. The observed peak enhancement and spectral shape are in good agreement with model predictions. Peak absorption of about 25% is obtained for a 3—5μm device (see Fig. 8).

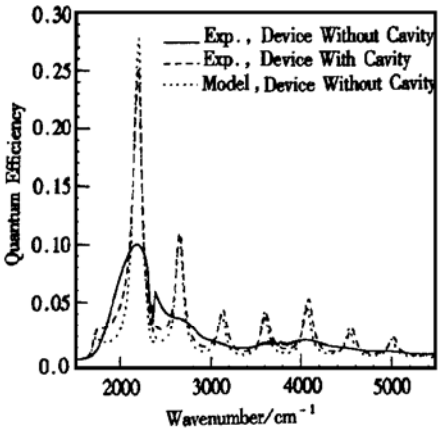

FIG. 8 A 5-μm Cutoff p-QWIP Spectra Experimental curve without cavity represents the double pass quantum efficiency. Observed spectrum on resonant cavity enhance device agrees with simulated quantum efficiency.

7 Conclusions

In this brief review, we presented the basic design rules for a standard n-type GaAs/AlGaAs QWIP. We discussed a few promising research directions for further investigation. For even longer term research, the quantum dot infrared photodetector[41] has the potential of normal incidence and high operating temperature (due to the expected long carrier lifetime), but it is not clear that the dot density can be controlled and increased to the point resulting in high absorption.

Acknowledgements I have benefited greatly from many discussions and collaborations over the years with fellow researchers in the field. Thanks are due to M. Buchanan for fabricating all the devices, to Z. R. Wasilewski for growing the highest quality wafers by MBE, to all the research associates (former and present), colleagues, and technicians. I am also extremely grateful to the continued funding provided by DND-DREV, started about a decade ago.

References

[1] H. C. Liu, Intersubband Transition in Quantum Wells: Physics and Device Applications I, Semiconductors and Semimetals, Academic Press, San Diego, Edited by H. C. Liu and F. Capasso, 2000, **62**: 126—196.

[2] S. D. Gunapala and S. V. Bandara, Semiconductors and Semimetals, 2000, **62**: 197—282.

[3] M. Helm, Semiconductors and Semimetals, 2000, **62**: 1—99.

[4] H. C. Liu, Z. R. Wasilewski, M. Buchanan and H. Chu, Appl. Phys. Lett., 1993, **63**: 761.

[5] Z. R. Wasilewski, H. C. Liu and M. Buchanan, J. Vac. Sci. Technol. B, 1994, **12**: 1273.

[6] S. K. H. Sim, H. C. Liu, A. Shen, M. Gao, K. F. Lee, M. Buchanan, Y. Ohno, H. Ohno and E. H. Li, Infrared Phys. Technol. (in press).

[7] D. Mandelik, M. Schniederman, V. Umansky and I. Bar-Joseph, Appl. Phys. Lett., 2001, **78**: 472.

[8] K. Nonaka, Jpn. Patent 4-364072, 1992.

[9] H. C. Liu, J. Li, Z. R. Wasilewski and M. Buchanan, Electron. Lett., 1995, **31**: 832.

[10] J. Y. Andersson and L. Lundqvist, Appl. Phys. Lett., 1991, **59**: 857.

[11] V. Ryzhii, M. Ershov, M. Ryzhii and I. Khmyrova, Jpn. J. Appl. Phys., 1995, **34**: L38.

[12] H. C. Liu, L. B. Allard, M. Buchanan and Z. R. Wasilewski, Electron. Lett., 1997, **33**: 379.

[13] V. Ryzhii, H. C. Liu, I. Khmyrova and M. Ryzhii, IEEE J. Quantum Electron., 1997, **33**: 1527.

[14] M. Ershov, H. C. Liu and L. M. Schmitt, J. Appl. Phys., 1997, **82**: 1446.

[15] L. B. Allard, H. C. Liu, M. Buchanan and Z. R. Wasilewski, Appl. Phys. Lett., 1997, **70**: 2784.

[16] E. Dupont, H. C. Liu, M. Buchanan, Z. R. Wasilewski, D. St-Germain and P. Chevrette, Appl. Phys. Lett., 1999, **75**: 563.

[17] H. C. Liu, M. Gao and P. Poole, Electron. Lett., 2000, **36**: 1300.

[18] E. R. Brown and K. A. McIntosh, United States Patent 5 304 805, 1994.

[19] R. Paiella, F. Capasso, C. Gmachl, D. L. Sivco, J. N. Baillargeon, A. L. Hutchinson, A. Y. Cho and H. C. Liu, Science

2000, **290**: 1739.

[20] R. Paiella, F. Capasso, C. Gmachl, H. Y. Hwang, D. L. Sivco, A. L. Hutchinson, A. Y. Cho and H. C. Liu, Appl. Phys. Lett., 2000, **77**: 169.

[21] H. C. Liu, J. Li, E. R. Brown, K. A. McIntosh, K. B. Nichols and M. J. Manfra, Appl. Phys. Lett., 1995, **67**: 1594.

[22] H. C. Liu, G. E. Jenkins, E. R. Brown, K. A. McIntosh, K. B. Nichols and M. J. Manfra, IEEE Electron Device Lett., 1995, **16**: 253.

[23] H. Schneider, C. Schönbein, G. Bihlmann, P. van Son and H. Sigg, Appl. Phys. Lett., 1997, **70**: 1602.

[24] B. F. Levine, K. K. Choi, C. G. Bethea, J. Walker and R. J. Malik, Appl. Phys. Lett., 1987, **50**: 1092.

[25] A. Köck, E. Gornik, G. Abstreiter, G. Böhm, M. Walther and G. Weimann, Appl. Phys. Lett., 1992, **60**: 2011.

[26] Ph. Bois, E. Costard, J. Y. Duboz and J. Nagle, SPIE, 1997, **3061**: 764.

[27] E. Costard, P. Bois, F. Audier and E. Herniou, SPIE, 1998, **3436**: 228.

[28] H. C. Liu, J. Li, J. R. Thompson, Z. R. Wasilewski, M. Buchanan and J. G. Simmons, IEEE Electron Device Lett., 1993, **14**: 566.

[29] L. C. Lenchyshyn, H. C. Liu, M. Buchanan and Z. R. Wasilewski, J. Appl. Phys., 1996, **79**: 8091.

[30] E. Martinet, E. Rosencher, F. Luc, Ph. Bois, E. Costard and S. Delaitre, Appl. Phys. Lett., 1992, **61**: 246.

[31] H. C. Liu, C. Y. Song, E. Dupont, P. Poole, P. W. Wilson, B. J. Robinson and D. A. Thompson, Electron. Lett., 1999, **35**: 2055.

[32] H. C. Liu, C. Y. Song, A. Shen, M. Gao, Z. R. Wasilewski and M. Buchanan, Appl. Phys. Lett., 2000, **77**: 2437.

[33] H. Schneider, C. Schönbein and G. Bihlmann, Appl. Phys. Lett., 1996, **68**: 1832.

[34] G. Sarusi, B. F. Levine, S. J. Pearton, K. M. S. Bandara and R. E. Leibenguth, Appl. Phys. Lett., 1994, **64**: 960.

[35] B. Xing and H. C. Liu, J. Appl. Phys., 1996, **80**: 1214.

[36] F. Szmulowicz and G. J. Brown, Phys. Rev. B, 1995, **51**: 13203.

[37] H. C. Liu, F. Szmulowicz, Z. R. Wasilewski, M. Buchanan and G. J. Brown, J. Appl. Phys., 1999, **85**: 2972.

[38] A. Shen, H. C. Liu, F. Szmulowicz, M. Buchanan, M. Gao, G. J. Brown and J. Ehret, J. Appl. Phys., 1999, **86**: 5232.

[39] A. Shen, H. C. Liu, M. Buchanan, M. Gao, F. Szmulowicz, G. J. Brown and J. Ehret, J. Vac. Sci. Technol. A, 2000, **18**: 601.

[40] A. Shen, H. C. Liu, M. Gao, M. Buchanan, E. Dupont, J. Ehret, G. J. Brown and F. Szmulowicz, Appl. Phys. Lett., 2000, **77**: 2400.

[41] H. C. Liu, M. Gao, J. McCaffrey, Z. R. Wasilewski and S. Fafard, Appl. Phys. Lett., 2000, **78**: 79.